

The Neurophysiological Bases of Cognitive Computation Using Rough Set Theory

Andrzej W. Przybyszewski

Department of Neurology, University of Massachusetts Medical Center,
Worcester, MA US

and

Department of Psychology, McGill University, Montreal, Canada

Andrzej.Prybyszewski@umassmed.edu

<http://www.umassmed.edu/neurology/faculty/Przybyszewski.cfm>

Abstract. A popular view is that the brain works in a similar way to a digital computer or a Universal Turing Machine by processing symbols. Psychophysical experiments and our amazing capability to recognize complex objects (like faces) in different light and context conditions argue against symbolic representation and suggest that concept representation related to similarities may be a more appropriate model of brain function. In present work, by looking into anatomical and neurophysiological basis of how we classify objects shapes, we propose to describe computational properties of the brain by rough set theory (Pawlak, 1992 [1]). Concepts representing objects physical properties in variable environment are weak (not precise), but psychophysical space shows precise object categorizations. We estimate brain expertise in classifications of the object's components by analyzing single cell responses in the area responsible for simple shape recognition ([2]). Our model is based on the receptive field properties of neurons in different visual areas: thalamus, V1 and V4 and on feedforward (FF) and feedback (FB) interactions between them. The FF pathways combine properties extracted in each area into a vast number of hypothetical objects by using "driver logical rules", in contrast to "modulator logical rules" of the FB pathways. The FB pathways function may help to change weak concepts of objects physical properties into their crisp classification in psychophysical space.

Keywords: imprecise computation, bottom-up, top-down processes, neuronal activity.

1 Introduction

Humans can effortlessly recognize objects as complex as faces even if they have never seen them in a particular context before. We are perceptually insensitive to the exact properties of an objects part, but the same parts in different configurations or contexts may result in opposite effects, much like the Thatcher effect. Psychophysical experiments related to complex object and faces categorization show that object recognition is based on incomplete information about an objects parts.

One of the most popular models based on psychophysical experiments is the geon model related to the Recognition-by-components (RBC) theory [3]. A geon can be structurally described (GSD) as a two-dimensional representation of an arrangement of parts, each specified in terms of its non-accidental characterization and the relations amongst these parts [3]. Across objects, the parts (geons, or geometric icons) can differ in their nonaccidental properties (NAP). NAP are properties that do not change with small depth rotations of an object. The presence or absence of NAP of some geons or the different relations between them is the basis for discrimination of viewpoint invariant objects [3]. Consequently, complex objects can be described by a simple “alphabet” by utilizing a small set of structural primitive geons. However, RBC theory not only does not attempt to describe a complex, real scene by an alphabet of geons, but it is also incomplete, failing to distinguish many real objects.

Such experiments suggest that in every day life we not only perform object classifications based solely on partial information about an object, but that we also make accessible information about variations in that object’s parts, such as its rotation or our viewpoint, indiscernible. An exact, crisp description (a set of values) of all the attributes of an object is therefore not only impossible because of the limitations of our visual system (such as a small area of sharp image, short perception time associated with the eye fixation period (see below), etc.), but also because we would like to identify the same object under different light conditions, contexts, localizations, rotations, etc. These difficulties in the context of our amazing capabilities in face and facial expression recognition led us (Prof. Zdzislaw Pawlak, Prof. Lech Polkowski, Prof. Andrzej Skowron, and myself) to discuss the application of rough set theory in order to find logical rules for complex object categorizations (the face project). Below I will present my summary regarding several points of our discussion.

As mentioned above, psychophysical and neurophysiological limitations led us to conclude that the brain-as-an-expert in complex object recognition may use vague concepts to process approximate information about a perceived object. Pawlak [1] proposed characterizing these concepts by their upper and lower approximations. The difference between the upper and lower approximations of a set of objects with related attributes is called its boundary region. Using the above characterizations, the concept of vagueness can be precisely expressed by the boundary region of a set. If a boundary region of a set is empty, the upper and lower approximations of the set are equal and the set is crisp (classical set theory). In this case, we can clearly classify the object on the basis of its properties as recognizable (a member of the set; logical value=1) or not recognizable (not a member of the set; logical value=0).

Crisp set also represents the classical approach to psychophysical experiments where near the limit of our vision, a subject can sometimes see the object and sometimes cannot. On the basis of averaging experimental results, we say that if the chance of seeing the object is over 50 % then the object is visible, and if it is below 50 %, then the object is not visible. The spectrum of an objects visibility is reduced to two values of a logical state: visible or not visible.

If the boundary region of a set is not empty, however, the set is rough and one can estimate the degree to which an object belongs to a set, or in other words, the precision with which the object is recognized. I claim that there are neurophysiological mechanisms in the brain responsible for shrinking the boundary regions along different dimensions in various visual areas of the brain. I describe these mechanisms with an example of the hierarchical structure: from the thalamus to area V4, the part of visual system responsible for simple shape discrimination. The thalamus classification characterizes an object by parts and questions how accurate divisions are using the rough inclusion relation or the rule that determines whether points are part of an object (Lesniewski mereology). For example, in order to find an object's contours, the surround portion of the LGNs receptive field should be outside of the object (see below for a more detailed analysis). In other visual areas such as V1, objects are partly described by oriented lines. More detailed measurements (see below) of area V1 receptive fields show many deviations from their sensitivity to only a single oriented edge. Their size for example, increases when light intensity decreases and it also depends on the mapping stimulus (i.e. dots vs. grating). Area V4 classifies objects to an extent as simple shapes coded in its neurons. For example, the mean size of the receptive field in area V4 is about 6 deg that means that there is partial overlap between an objects size and a single cell receptive field (RF) in area V4. Therefore, the relationship between object and receptive field in most situations is not crisp.

The famous mathematician Lukasiewicz's once asked whether or not it was true that "Jan will be in Warsaw next year?" This question initiated a course of research related to uncertainty using multi-valued logic. The activities of our sensory and motor systems are also related to uncertainty. In sensory-related motion, our eyes are constantly moving, with brief periods of fixation during which reliable information about interesting objects must be obtained and depending on the information received, a decision about the next eye movement must be made. The brain is continually verifying sensory information with predictions that are related to assumptions about the environment and possible object properties. Similarly, in a constantly changing environment, the brain has to make calculations and predictions with regards to behavior about how to meet or catch an object with uncertain properties and movement trajectories. These predictions are verified and corrected during each movement. We can therefore paraphrase Lukasiewicz's sentence in relation to subconsciously-made brain decisions as: "If I move my eyes to the right in the next 100 ms, will I know that it is Jan's face?" or "If I correct my hand trajectory in the next 50 ms will I catch the ball?"

The main purpose of this paper is to relate anatomical and neurophysiological brain properties to object categorization. In order to quantify the neurophysiological data and model perception, we will use rough set theory [1]. The complexity of the brain and many different methods of measurement generated huge amounts of data that led to unclear and contradictory theories. This work therefore compares data from the literature with data from our

electrophysiological experiments using rough set theory and multi-valued logic. Using these precise descriptions, we would like to find closer connections between the electrophysiological and AI (expert) systems, as well as describe our results using psychological language.

Like Pawlak [1], we define an information system as $S = (U, A)$, where U is a set of objects and A is set of attributes. If $a \in A$, $u \in U$ the value $a(u)$ is a unique element of V_a (a value set of the attribute a). In agreement with the Leibniz principle we assume that objects are completely determined by their set of properties, meaning that attributes map objects to a set of attributes values. The indiscernibility relation of any subset B of A , or $IND(B)$, is defined [1] as the equivalence relation whose elements are the sets $u : b(u) = v$ as v varies in V_b , and $[u]_B$ - the equivalence class of u form B -*elementary granule*. The concept $X \subseteq U$ is B -*definable* if for each $u \in U$ either $[u]_B \subseteq X$ or $[u]_B \subseteq U - X$. $\underline{B}X = \{u \in U : [u]_B \subseteq X\}$ is a lower approximation of X . The concept $X \subseteq U$ is B -*indefinable* if exists such $u \in U$ that $[u]_B \cap X \neq \emptyset$. $\overline{B}X = \{u \in U : [u]_B \cap X \neq \emptyset\}$ is an upper approximation of X . The set $BN_B(X) = \overline{B}X - \underline{B}X$ will be referred to as the B -*boundary region* of X . If the boundary region of X is the empty set then X is exact (crisp) with respect to B ; otherwise if $BN_B(X) \neq \emptyset$ X is not exact (rough) with respect to B .

In this paper, the universe U is a set of simple visual patterns that we used in our experiments [2, 4, 5], and which can be divided into equivalent indiscernibility classes related to their physically measured, computer generated attributes or B -*elementary granules*, where $B \subseteq A$.

The purpose of our research is to find how these objects are classified in the brain. We will therefore modify, after [1], the definition of the information system as $S = (U, C, D)$ where C and D are condition and decision attributes respectively. Decision attributes will classify elementary granules in accordance with neurological responses from a specific area of the visual brain. From a cognitive perspective, the percept of the object is classified into different categories in different visual areas, leading to different decisions (actions). The information system is equivalent to the decision table in which each object $u \in U$ is characterized by a series of the condition attributes and one decision attribute. The information system can be also seen as agents' intelligence where condition attributes described agents' percepts and decision attributes are related to the agents' action [6].

This work investigates the responses of cells in the thalamus that will divide all equivalent pattern classes into LGN-elementary granules $[u]_{LGN}$, as well as the responses of cells in area V1 that will divide all patterns into V1-elementary granules $[u]_{V1}$, and the responses of cells in area V4 that will divide all patterns into V4-elementary granules $[u]_{V4}$. All neurons in these areas are sensitive to certain attributes of the stimulus, such as space localization, but each area also performs distinct pattern classification. In consequence, one B -*elementary granule* will be classified in many different ways by neurons in different areas. All these granules: $[u]_{LGN}$, $[u]_{V1}$, $[u]_{V4}$ are exact. They cover the visual field in a unique way for a fixed eye position, even if the receptive

fields of different cells overlap. Relationships between granules from different areas are rough, however, meaning that granules containing information related to feedforward connections $[u]_{LGN} \subseteq [u]_{V1} \subseteq [u]_{V4}$ and to feedback pathways: $[u]_{V4} \subseteq U_{s \in S}[u]_{V1}^s \subseteq U_{s \in S}[u]_{LGN}^s$ are rough inclusions, where $U_{s \in S}$ is mereological sum of all granules covering area of the the V4 neuron. As we will show below, each pathway obeys different logical rules. Our hypothesis is that the brain uses a hierarchical multi-level classification in order to find different important invariances at each level. These invariances may help to classify different presentations of the same object that, in different conditions, may lack or show changes in some of its parts.

Our model describes neurophysiological data in rough set theory [1] language and suggests that in order to classify complex objects the brain uses multi-valued logic, granular knowledge and rough mereology.

2 Basic Concepts

2.1 Objects' (stimuli) Attributes and Classification of the Brain Responses

We will represent our experimental data [2] in the following tables (Tabs. 1-5). In the first column are neural measurements. Neurons are identified using numbers related to a collection of figures in [2] concatenated with the cell number. Additional letters (a, b, \dots) denotes different measurements of the same cell. For example, $11a$ denotes the first measurement of a neuron numbered 1 Fig. 1, $11b$ the second measurement, etc. Simple stimuli properties are as characterized as follows: Most of our analysis will be related to data from Pollen et al. [2].

1. Orientation in degrees appears in the column labeled o , and orientation bandwidth is ob .
2. spatial frequency is denoted as sf , spatial frequency bandwidth is sfb
3. x -axis position is denoted by xp and the range of x-positions is xpr
4. y -axis position is denoted by yp and the range of y-positions is ypr
5. x -axis stimulus size is denoted by xs
6. y -axis stimulus size is denoted by ys
7. stimulus shape is denoted by s , values of s are following: for grating $s = 1$, for vertical bar $s = 2$, for horizontal bar $s = 3$, for disc $s = 4$, for annulus $s = 5$, for two stimuli $s = 22$ - two vertical bars, etc.

Stimulus attributes can be express as:

$$B = \{o, ob, sf, sfb, xp, xpr, yp, ypr, xs, ys, s\}.$$

Generally, we divide all cell responses into n ranges, but in this paper, for simplicity, we use three ranges of the neural responses. Activity below the threshold in between 10 and 20 spikes/s is defined as a *category 0* cell response. Activity above the threshold is defined as *category 1*, and activity above $30 - 40$ spikes/s as *category 2*. We analyze only the dominant component of the cell response,

which in LGN and simple V1 cells is *linear* (the first harmonic F_1) and in the complex V1 cell and in V4 cell is *nonlinear* (related to F_0 or the mean changes in the neuronal discharges). The reason for choosing the minimum significant cell activity of $10 - 20$ spikes/s is as follows: during normal activity our eyes are constantly moving. The fixation periods are between 100 and 300ms, similar to those of monkeys. Assuming that a single neuron, in order to give reliable information about an object, must fire a minimum of $2-3$ spikes during the eye fixation period, we obtain a minimum frequency of 10 to 20 spikes/s. We assume that these discharges are determined by the bottom-up information (hypothesis testing) and that they are related to the sensory information about an object's form. The brain is constantly making predictions, which are verified by comparing them with sensory information. These tests are performed in a positive feedback loop [4, 7]. If prediction is in agreement with the hypothesis, we assume that activity of the cell increases approximately twofold similarly to the strength of the feedback from V1 to LGN [4]. This increased activity is related to category 2. Cell responses (r) are divided into 3 ranges:

- category 0:** activity below the threshold $10 - 20$ sp/s labeled by r_0 ;
- category 1:** activity above the threshold labeled by r_1 ;
- category 2:** activity above $30 - 40$ sp/s labeled by r_2 .

2.2 Logic of the Anatomical Connections

As it was mentioned above, our model consists of three interconnected visual areas. Their connections can be divided into feedforward (FF) and feedback (FB) pathways. We have proposed [7] that the role of the FF pathways is to test the hypothesis about stimulus attributes and the function of the FB pathways is to make predictions. Below, we suggest that the different anatomical properties of the FB and FF pathways may determine their different logical rules. We define LGN_i , as LGN i -cell attributes for cells $i = 1, \dots, n$, $V1_j$ as primary visual cortex j -cell attributes for cells $j = 1, \dots, m$, and $V4_k$ as area V4 attributes for cells $k = 1, \dots, l$. The specific stimulus attributes for a single cell can be found in the neurophysiological experiment by recording cell responses to the set of various test stimuli. As we have mentioned above, cell responses are divided into several (here 3) ranges, which will define several granules for each cell. It is different from the classical receptive field definition, which assumes that the cell responds (*logical value 1*) or does not respond (*logical value 0*) to the stimulus with certain attributes. In the classical electrophysiological approach all receptive field granules are crisp. In our approach, cell responses below the threshold (r_0), have logical value 0, whereas the maximum cell responses (r_2), have a logical value 1. We will introduce cell responses between r_0 and r_2 , in this paper there is only one value, r_1 . The physiological interpretation of cell responses between the threshold and the maximum response may be related to the influence of the feedback or horizontal pathways. We assume that the tuning of each structure is different and we will look for decision rules in each level that give responses r_1 and r_2 . For example, we assume that r_1 means that the local

structure is tuned to the attributes of the stimulus and such granule for j cell in area V1 will be define as $[u]_{1V1j}$.

Decision Rules for a single neuron. Each neuron in the central nervous system sums up its synaptic inputs as a postsynaptic excitatory (*EPSPs*) and/or inhibitory (*IPSPs*) potentials that may cause its membrane potential to exceed the threshold and to generate an action potential. A single neuron approximates collective (thousands of interacting synapses with different weights) input information to the distributive one (unique decision in a single output). In principle, a single spike (action potential) can be seen as a decision of the neuron, but in this work we will not take into account internal dynamics of the system and therefore we will estimate neuronal activity as spikes mean frequency (as described above). This complex synaptic potential summation process is related in sensory (here only visual) systems with the receptive field properties of each neuron. Below we will show how neurons in different parts of the brain change visual information in their receptive fields into decisions.

Decision Rules for LGN. Each LGN cell is sensitive to luminance changes in a small part of the visual field called the receptive field (RF). The cells in the LGN have the concentric center-surround shapes of their RFs, which are similar to that in the retinal ganglion cells [8]. We will consider only on- and off type RFs. The on - (off) type cells increase (decrease) their activity by an increase of the light luminance in their receptive field center and/or decrease of the light luminance in the RF surround (Fig. 1). Below are examples of the decision rules for on-, and off-type LGN cells with their RF positions: xp_0, yp_0 . We assume that there is no positive feedback from higher areas therefore their maximum responses are r_1 .

DR_LGN_1:

$$xp_0 \wedge yp_0 \wedge xs_{0.1} \wedge ys_{0.1} \wedge s_4 \rightarrow r_1 \quad (1)$$

DR_LGN_2:

$$xp_0 \wedge yp_0 \wedge xs_{0.3} \wedge ys_{0.3} \wedge s_5 \rightarrow r_1 \quad (2)$$

which we interpret that the changes in the luminance of the light spot s_4 that covers the RF center (the first rule) or annulus s_5 that covers the RF surround (the second rule) gives neuronal response r_1 . We assume that other stimulus parameters like contrast, speed and frequency of luminance changes, etc. are constant and optimal, and that the cell is linear and therefore we measure response of the cell activity synchronized with the stimulus changes (the first harmonic). Depending on the cell type the phase shift between stimulus and the response is near 0 or $180deg$ if we do not take into account the phase shift related to the response delay. Instead, using light spots or annuli one can use a single, modulated with the drifting grating, circular patch covering the classical RF. By changing the spatial frequency of the drifting grating one can stimulate only the RF center for high spatial frequencies or center and surround for lower spatial frequencies, which gives the following decision rule:

DR_LGN_3:

$$xp_0 \wedge yp_0 \wedge xs_{0.3} \wedge ys_{0.3} \wedge sf_{0.4} \rightarrow r_1 \quad (3)$$

where for example: $sf = 0.4c/d$ stimulates RF center and surround, $sf \geq 1c/d$ stimulates RF center only. Notice that in agreement with the above rules eqs. (1-3) LGN cells do not differentiate between light spot, light annulus, and patch modulated with grating. All these different objects represent the same LGN-elementary granule.

Decision Rules for area V1. In the primary visual cortex (area V1) neurons obtain a new property: sensitivity to the stimulus orientation, which is not observed in lower areas: retina or LGN [9]. The area V1 has at least two different cell types: simple and complex. They can be characterized by spatial relationships between their incremental (on) and decremental (off) subfields. In a simple cell on and off subfields are separated, whereas a complex cell is characterized by the overlap of its subfields. In consequence simple cells are linear (the first harmonic dominates in their responses: $F1/F0 > 1$), whereas complex cells are nonlinear ($F1/F0 < 1$). The classical V1 RF properties can be found using small flashing light spots, moving white or dark bars or gratings. We will give an example of the decision rules for the RF mapped with the moving white and dark bars [5]. A moving white bar gives the following decision rule:

DR_V1_1:

$$xp_i \wedge yp_0 \wedge xs_k \wedge ys_1 \wedge s_2 \rightarrow r_1 \quad (4)$$

The decision rule for a moving dark bar is given as:

DR_V1_2:

$$xp_j \wedge yp_0 \wedge xs_l \wedge ys_1 \wedge s_2 \rightarrow r_1 \quad (5)$$

where xp_i is the x-position of the incremental subfield, where xp_j is the x-position of the decremental subfield, yp_0 is the y-position of the both subfields, xs_k , xs_l , ys_1 are horizontal and vertical sizes of the RF subfields, and s_2 is a vertical bar which means that this cell is tuned to the vertical orientation. We have skipped other stimulus attributes like movement velocity, direction, amplitude, etc. For simplicity we assume that the cell is not direction sensitive, it gives the same responses to both direction of bar movement and to the dark and light bars and that cell responses are symmetric around the x middle position (xp). An overlap index [10] is defined as:

$$OI = \frac{0.5(xs_k + xs_l) - |xp_i - xp_j|}{0.5(xs_k + xs_l) + |xp_i - xp_j|}$$

OI compares sizes of increment (xs_k) and decrement (xs_l) subfields to their separation ($|xp_i - xp_j|$). After [11], if $OI \leq 0.3$ ("non-overlapping" subfields) it is the simple cell with dominating first harmonic response (linear) and r_1 is the amplitude of the first harmonic. If $OI \geq 0.5$ (overlapping subfields), it is the complex cell with dominating $F0$ response (nonlinear) and r_1 are changes in the mean cell activity. Hubel and Wiesel [9] have proposed that the complex

cell RF is created by convergence of several simple cells in a similar way like V1 RF properties are related to RF of LGN cells (Fig. 1). However, there is recent experimental evidence that the nonlinearity of the complex cell RF may be related to the feedback or horizontal connections [12].

Decision Rules for area V4. The properties of the RFs in area V4 are more complex than that in area V1 or in the LGN and in most cases they are nonlinear. It is not clear what exactly optimal stimuli for cells in V4 are, but a popular hypothesis states that the V4 cells code the simple, robust shapes. Below there is an example from [13] of the decision rules for a narrow (0.4 deg) and long (4 deg) horizontal or vertical bars placed in different positions of area V4 RF:

DR_V4_1:

$$o_0 \wedge ypr_m \wedge (yp_{-2.2} \vee yp_{0.15}) \wedge xs_4 \wedge ys_{0.4} \rightarrow r_2 \tag{6}$$

DR_V4_2:

$$o_{90} \wedge xpr_m \wedge (xp_{-0.6} \vee xp_{1.3}) \wedge xs_{0.4} \wedge ys_4 \rightarrow r_1 \tag{7}$$

The first rule relates area V4 cell responses to a moving horizontal bar (o_0) and the stimulus in the second rule is a moving vertical bar (o_{90}), ypr_m , xpr_m have meaning of the tolerance for the y or x bar positions (more details in the Result section). The horizontal bar placed narrowly in two different y -positions ($yp_{-2.2}, yp_{0.15}$) gives strong cell responses (**DR_V4_1**), and the vertical bar placed with wide range in two different x -positions ($xp_{-0.6}, xp_{1.3}$) gives medium cell responses.

Decision Rules for feedforward connections from LGN \rightarrow V1. Thalamic axons target specific cells in layers 4 and 6 of the primary visual cortex (V1). Generally we assume that there is a linear summation of LGN cells (approximately 10 – 100 of them [14]) to one V1 cell. It was proposed [9] that the LGN cells determine the orientation of the V1 cell in the following way: LGN cells which have a direct synaptic connection to V1 neurons have their receptive fields arranged along a straight line on the retina (Fig. 1). In this Hubel and Wiesel [9] classical model the major assumption is that activity of all (four in Fig. 1) LGN cells is necessary for a V1 cell to be sensitive to the specific stimulus (oriented light bar). This principle determines syntax of the LGN to V1 decision rule, by using logical and meaning that if one LGN cell does not respond then there is no V1 cell response. After Sherman and Guillery [15] we will call such inputs drivers. Alonso et al. [14] showed that there is a high specificity between RF properties of the LGN cells which have monosynaptic connections to a V1 simple cell. This precision goes beyond simple retinotopy and includes such RF properties as RF sign, timing, subregion strength and sign [14]. The decision rule for the feedforward LGN to V1 connections are following:

DR_LGN_V1_1:

$$r_1^{LGN}(x_i, y_i) \wedge r_1^{LGN}(x_{i+1}, y_i) \wedge \dots \wedge r_1^{LGN}(x_{i+n}, y_i) \rightarrow r_1^{V1} \tag{8}$$

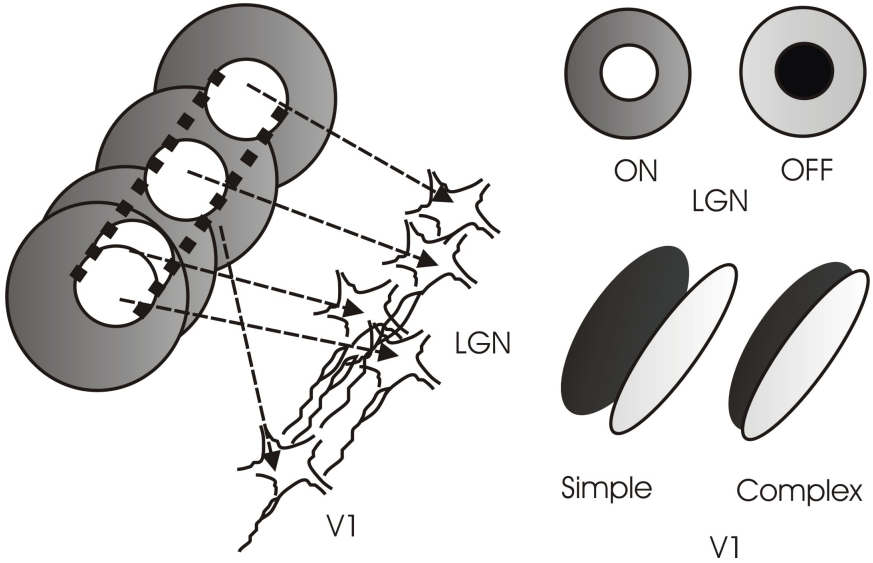


Fig. 1. On the left: modified schematic of the model proposed by [9]. Four LGN cells with circular receptive fields arranged along a straight line on the retina have direct synaptic connection to V1 neuron. This V1 neuron is orientation sensitive as marked by the thick, interrupted lines. On the right: receptive fields of two types of LGN cells, and two types of area V1 cells.

DR_LGN_V1.2:

$$r_1^{LGN}(x_i, y_i) \wedge r_1^{LGN}(x_{i+1}, y_{i+1}) \wedge \dots \wedge r_1^{LGN}(x_{i+n}, y_{i+1}) \rightarrow r_1^{V1} \quad (9)$$

where the first rule determines response of cells in V1 with optimal horizontal orientation, and the second rule says that the optimal orientation is 45 degrees; (x_i, y_i) is the localization of the RF in x-y Euclidian coordinates of the visual field. Notice that these rules assume that V1 RF is completely determined by the FF pathway from the LGN.

Decision Rules for feedback connections from V1→LGN. There are several papers showing the existence of the feedback connections from V1 to LGN [16-20]. In [20], authors have quantitatively compared the visuotopic extent of geniculate feedforward afferents to V1 with the size of the RF center and surround of neurons in V1 input layers and the visuotopic extent of V1 feedback connections to the LGN with the RF size of cells in V1. Area V1 feedback connections restrict their influence to LGN regions visuotopically coextensive with the size of the classical RF of V1 layer 6 cells and commensurate with the LGN region from which they receive feedforward connections. In agreement with [15] we will denote feedback inputs modulators with following decision rules:

DR_V1_LGN_1:

$$(r_1^{V1} \vee r_1^{LGN}(x_i, y_i)), (r_1^{V1} \vee r_1^{LGN}(x_i, y_{i+1})), (r_1^{V1} \vee r_1^{LGN}(x_{i+1}, y_{i+1})), \dots \\ \dots, r_1^{LGN}(x_{i+2n}, y_{i+2n})) \rightarrow r_2^{LGN} \tag{10}$$

This rule says that when the activity of a particular V1 cell is in agreement with activity in some LGN cells their responses increase from r_1 to r_2 , and $r_1^{LGN}(x_i, y_i)$ means r_1 response of LGN cell with coordination (x_i, y_i) in the visual field, and r_2^{LGN} means r_2 response of all LGN cells in the decision rules which activity was coincidental with the feedback excitation, it is a pattern of LGN cells activity.

Decision Rules for feedforward connections V1 → V4. There are relatively small direct connections from V1 to V4 bypassing area V2 [20], but we also must take into account V1 to V2 [21] and V2 to V4 connections, which are highly organized but variable, especially in V4 [22] feedforward connections. We simplify that V2 has similar properties to V1 but have a larger size of the RF. We assume that, like from the retina to LGN and from LGN to V1 direct or indirect connections from V1 to V4 provide driver input and fulfill the following decision rules:

DR_V1_V4_1:

$$r_1^{V1}(x_i, y_i) \wedge r_1^{V1}(x_{i+1}, y_i) \wedge \dots \wedge r_1^{V1}(x_{i+n}, y_i) \rightarrow r_1^{V4} \tag{11}$$

DR_V1_V4_2:

$$r_1^{V1}(x_i, y_i) \wedge r_1^{V1}(x_{i+1}, y_{i+j}) \wedge \dots \wedge r_1^{V1}(x_{i+n}, y_{i+m}) \rightarrow r_1^{V4} \tag{12}$$

We assume that, the RF in area V4 sums up driver inputs from regions in the areas V1 and V2 of cells with highly specific RF properties, not only retinotopically correlated.

Decision Rules for feedback connections from V4→V1. Anterograde anatomical tracing [23] has shown axons backprojecting from area V4 directly to area V1 or sometimes with branches in area V2. Axons of V4 cells span in area V1 in large territories with most terminations in layer 1, which can be either distinct clusters or in linear arrays. These specific for each axon branches determine decision rules that will have similar syntax (see below) but anatomical structure of the particular axon may introduce different semantics. Their anatomical structures maybe related to the specific receptive field properties of different V4 cells. Distinct clusters may have terminals on V1 cells near pinwheel centers (cells with different orientations arranged radially), whereas a linear array of terminals may be connected to V1 neurons with similar orientation preference. In consequence, some parts of the V4 RF would have preference for certain orientations and others may have preference for the certain locations but be more flexible to different orientations. This hypothesis is supported by recent intracellular recordings from neurons located near pinwheels centers which,

in contrast to other narrowly tuned neurons, showed subthreshold responses to all orientations [24]. However, neurons which have fixed orientation can change other properties of their receptive field like for example spatial frequency, therefore the feedback from area V4 can tune them to expected spatial details in the RF (M. Sur, Brenda Milner Symposium, 22 Sept. 2008, MNI McGill University, Montreal).

The V4 input modulates V1 cell in the following way:

DR_V4_V1_1:

$$(r_1^{V4} \vee r_1^{V1}(x_i, y_i)), (r_1^{V4} \vee r_1^{V1}(x_i, y_{i+1})), (r_1^{V4} \vee r_1^{V1}(x_{i+1}, y_{i+1})), \dots \\ \dots, (r_1^{V4} \vee r_1^{V1}(x_{i+n}, y_{i+m})) \rightarrow r_2^{V1} \quad (13)$$

Meaning of $r_1^{V1}(x_i, y_i)$ and r_2^{V1} are same as explained above for the V1 to LGN decision rule.

Decision Rules for feedback connections V4→LGN. Anterograde tracing from area V4 showed axons projecting to different layers of LGN and some of them also to the pulvinar [25] These axons have widespread terminal fields with branches non-uniformly spread about several millimeters (Fig. 2). Like descending axons in V1, axons from area V4 have within their LGN terminations, distinct clusters or linear branches (Fig. 2). These clusters and branches are characteristic for different axons and as it was mentioned above their differences may be related to different semantics in the decision rule below:

DR_V4_LGN_1:

$$(r_1^{V4} \vee r_1^{LGN}(x_i, y_i)), (r_1^{V4} \vee r_1^{LGN}(x_i, y_{i+1})), (r_1^{V4} \vee r_1^{LGN}(x_{i+1}, y_{i+1})), \dots \\ \dots, (r_1^{V4} \vee r_1^{LGN}(x_{i+n}, y_{i+m})) \rightarrow r_2^{LGN} \quad (14)$$

Meaning of $r_1^{LGN}(x_i, y_i)$ and r_2^{LGN} are same as explained above for the V1 to LGN decision rule.

Notice that interaction between FF and FB pathways extends a classical view that the brain as computer uses two-valued logic. This effect in psychophysics can be paraphrased as: “I see it but it does not fit my predictions”. In neurophysiology, we assume that a substructure could be optimally tuned to the stimulus but its activity does not fit to the FB predictions. Such interaction can be interpreted as the third logical value. If there is no stimulus, the response in the local structure should have a logical value 0, if stimulus is optimal for the local structure, it should have logical value $\frac{1}{2}$, and if it also is tuned to expectations of higher areas (positive feedback) then response should have logical value 1. Generally it becomes more complicated if we consider many interacting areas, but in this work we use only three-valued logic.

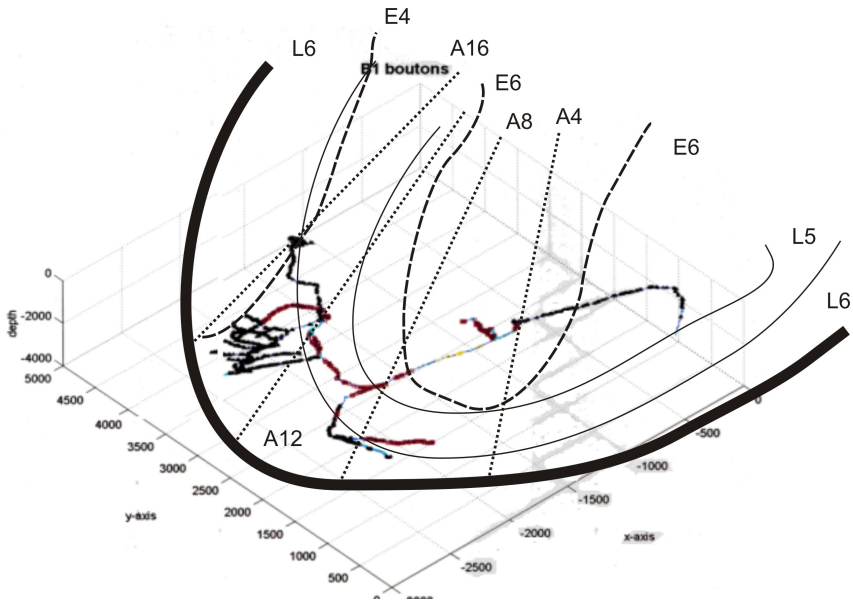


Fig. 2. Boutons of the descending axon from area V4 with terminals in different parvocellular layers of LGN: layer 6 in black, layer 5 in red, layer 4 in yellow. Total number of boutons for this and other axons was between 1150 and 2075. We estimated that it means that each descending V4 axon connects to approximately 500 to over 1000 LGN (mostly parvocellular) cells [25]. Thick lines outline LGN; thin lines shows layers 5 and 6, dotted line azimuth, and dashed lines show elevation of the visual field covered by the descending axon. This axon arborization extension has approximately V4 RF size.

3 Results

We have used our model as a basis for an analysis of the experimental data from the neurons recorded in the monkey's area V4 [2]. In [2], it was shown that the RF in V4 can be divided into several subfield that, stimulated separately, can give us the first approximation of the concept of the shape to which the cell is tuned [13]. We have also shown that subfields are tuned to stimuli with similar orientation [2]. In Fig. 3, we demonstrate that the receptive field subfields have not only similar preferred orientations but also spatial frequencies [2]. We have divided cell responses into three categories (see Methods) by horizontal lines in plots A-D of Fig. 3.

We have draw a line near spike frequency 17 spikes/s , which separates responses of category r_1 (above) from r_0 (below the threshold line). Horizontal lines plotted near spike frequency 34 spikes/s separate responses of category r_2 (above) from r_1 (below). The stimulus attributes related to these three response categories were extracted in the decision table (Table 1). We summarize results of our analysis in Figs. 3H and G from Table 1. Fig. 3H presents a schematic of a possible stimulus that would give medium cell responses (r_1). One can imagine

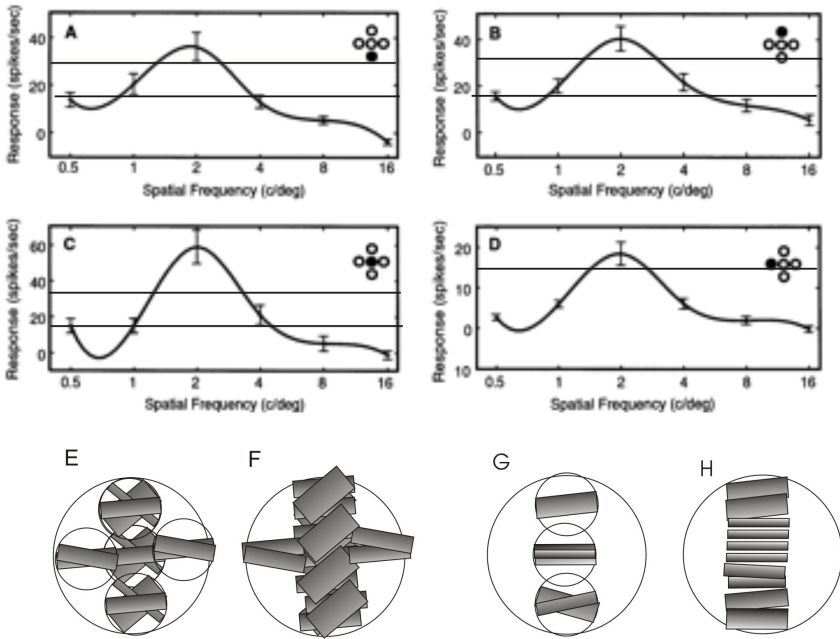


Fig. 3. Modified plots from [2]. Curves represent responses of V4 neurons to their RF subfields grating stimulations with different spatial frequencies (SF). (A-D) SF selectivity curves across RF with positions indicated in insets. The centers of tested subfields were 2 deg apart. (E-H) Schematic representation summarizing orientation and SF selectivity of subfields presented in A-D and in [2]. These figures are based on the decision table 1, for stimuli in E, F cell responses were r_1 , for stimuli in G, H cell responses were r_2 , (F) and (G) represent a possible stimulus configuration from schematics (E) and (F).

several classes of possible stimuli assuming that subfield responses will sum up linearly (for example see Fig. 3F). Fig. 3G shows a schematic of a possible stimulus set-up, which would give r_2 response that as we have assumed, is related not only to the local but also the global visual cortex tuning. One can notice that in the last case only subfields in the vertical row give strong independent responses (Fig. 3H).

We assign the narrow (ob_n), medium (ob_m), and wide (ob_w) orientation bandwidth as follows: ob_n if ($ob : 0 < ob < 50deg$), medium ob_m if ($ob : 50deg < ob < 100deg$), wide ob_w if ($ob : ob > 100deg$). We assign the narrow (sfb_n), medium (sfb_m), and wide (sfb_w) spatial frequency bandwidth: sfb_n if ($sfb : 0 < sfb < 2c/deg$), medium sfb_m if ($sfb : 2c/deg < sfb < 2.5c/deg$), wide sfb_w if ($sfb : sfb > 2.5c/deg$). For simplicity in the following decision rules, we assume that the subfields are not direction sensitive; therefore responses to stimulus orientation θ and $180 deg$ should be same.

Table 1. Decision table for one cell responses to subfields stimulation Fig. 3C-F and Fig.5 in [2]. Attributes $xpr, ypr, sf = 2c/deg, s$ are constant and they are not presented in the table. Cells 3* are from Fig. 3 in [2] and cells 5* are from Fig. 5 in [2] processed in Fig. 3.

<i>cell</i>	<i>o</i>	<i>ob</i>	<i>sfb</i>	<i>xp</i>	<i>yp</i>	<i>r</i>
3c	172	105	0	0	0	1
3c1	10	140	0	0	0	1
3c2	180	20	0	0	0	2
3d	172	105	0	0	-2	1
3d1	5	100	0	0	-2	1
3d2	180	50	0	0	-2	2
3e	180	0	0	-2	0	0
3f	170	100	0	0	2	1
3f1	10	140	0	0	2	1
3f2	333	16	0	0	2	2
5a	180	0	3	0	-2	1
5a1	180	0	0.9	0	-2	2
5b	180	0	3.2	0	2	1
5b1	180	0	1	0	2	2
5c	180	0	3	0	0	1
5c1	180	0	1.9	0	0	2
5d	180	0	0.8	0	0	1

Our results from the separate subfields stimulation study can be presented as the following decision rules:

DR_V4_3:

$$o_{180} \wedge sf_2 \wedge ((ob_w \wedge sfb_w \wedge xp_0 \wedge (yp_{-2} \vee yp_0 \vee yp_2))) \vee \vee (ob_n \wedge sfb_n \wedge yp_0 \wedge (xp_{-2} \vee xp_2)) \rightarrow r_1 \tag{15}$$

DR_V4_4:

$$o_{180} \wedge sf_2 \wedge ob_n \wedge sfb_n \wedge xp_0 \wedge (yp_{-2} \vee yp_0 \vee yp_2) \rightarrow r_2 \tag{16}$$

These decision rules can be interpreted as follows: disc shaped grating stimuli with wide bandwidths of orientations or spatial frequencies when placed along vertical axis of the receptive field evoke medium cell responses. However, similar discs when placed horizontally to the left or to the right from the middle of the RF, must have narrow orientation and spatial frequency to evoke medium cell responses. Only a narrowly tuned disc in spatial frequency and orientation placed vertically from the middle of the receptive field can evoke strong cell responses. Notice that Figs 3F and 3H show possible configurations of the optimal stimulus. This approach is similar to the assumption that an image of the object is initially represented in terms of the activation of a spatially arrayed set of multiscale, multioriented detectors like arrangements of simple cells in V1 (metric

templates in subordinate-level object classification of Lades et al. [26]). However, this approach does not take into account interactions between several stimuli, when more than one subfield is stimulated, and we will show below there is a strong nonlinear interaction between subfields. We analyzed experiments where the RF is stimulated at first with a single small vertical bar and later with two bars changing their horizontal positions. One example of V4 cell responses to thin (0.25 deg) vertical bars in different horizontal positions is shown in the upper left part of Fig. 4 (Fig. 4E). Cell response has maximum amplitude for the middle ($XPos = 0$) bar position along the x -axis. Cell responses are not symmetrical around 0. In Fig. 2F, the same cell (cell 61 in table 2) is tested with two bars. The first bar stays at the 0 position, while the second bar changes its position along x -axis. Cell responses show several maxima dividing the receptive field into four areas. However, this is not always the case as responses to two bars in another cell (cell 62 in table 2) show only two minima (Fig. 2G). Horizontal lines in plots of both figures divide cell responses into the three categories r_0 , r_1 , r_2 , which are related to the mean response frequency (see Methods). Stimuli attributes and cell responses classified into categories are shown in table 2 for cells in Fig. 4 and in table 3 for cells in Fig. 5.

We assign the narrow (xpr_n), medium (xpr_m), and wide (xpr_w) x position ranges as follows: xpr_n if ($xpr : 0 < xpr \leq 0.6$), medium xpr_m if ($xpr : 0.6 < xpr \leq 1.2$), wide xpr_w if ($xpr : xpr > 1.2$). We assign the narrow (ypr_n), medium (ypr_m), and wide (ypr_w) y position range: ypr_n if ($ypr : 0 < ypr \leq 1.2$), medium ypr_m if ($ypr : 1.2 < xpr \leq 1.6$), wide ypr_w if ($ypr : ypr > 1.6$).

On the basis of Fig. 3 and the decision table 2 (also compare with [18]) the one-bar study can be presented as the following decision rules:

DR_V4_5:

$$o_{90} \wedge xpr_n \wedge xp_{0.1} \wedge xs_{0.25} \wedge ys_{0.4} \rightarrow r_2 \quad (17)$$

DR_V4_6:

$$o_{90} \wedge xpr_w \wedge xp_{-0.2} \wedge xs_{0.25} \wedge ys_{0.4} \rightarrow r_1 \quad (18)$$

We interpret these rules that r_1 response in eq. (18) does not effectively involve the feedback to the lower areas: V1 and LGN. The descending V4 axons have excitatory synapses not only on relay cells in LGN and pyramidal cells in V1, but also on inhibitory interneurons in LGN and inhibitory double banquet cells in layer 2/3 of V1. As an effect of the feedback, only a narrow range of area V4 RF responded with a high r_2 activity to a single bar stimulus, whereas in the outside area excitatory and inhibitory feedback influences compensated each other.

On the basis of Fig. 4 the decision table, the two-bar horizontal interaction study can be presented as the following **Two-bar Decision Rules (DRT)**:

DRT_V4_1:

$$o_{90} \wedge xpr_n \wedge ((xp_{-1.9} \vee xp_{0.1} \vee xp_{1.5}) \wedge xs_{0.25} \wedge ys_{0.4})_1 \wedge (o_{90} \wedge xp_0 \wedge xs_{0.25} \wedge ys_{0.4})_0 \rightarrow r_2 \quad (19)$$

DRT_V4_2:

$$o_{90} \wedge xpr_m \wedge ((xp_{-1.8} \vee xp_{-0.4} \vee xp_{0.4} \vee xp_{1.2}) \wedge xs_{0.25} \wedge ys_{0.4})_1 \wedge \wedge (o_{90} \wedge xp_0 \wedge xs_{0.25} \wedge ys_{0.4})_0 \rightarrow r_1 \tag{20}$$

One-bar decision rules can be interpreted as follows: the narrow vertical bar evokes a strong response in the central positions, and medium responses in a larger area near the central position. Two-bar decision rules claim that: the cell responses to two bars are strong if one bar is in the middle of the RF (bar with index 0 in decision rules) and the second narrow bar (bar with index 1 in decision rules) is in the certain, specific positions in the RF eq. (19). But when the second bar is in less precise positions, cell responses became weaker eq. (20). Responses of other cells are sensitive to other bar positions (Fig. 4G). These differences could be correlated with anatomical variability of the descending

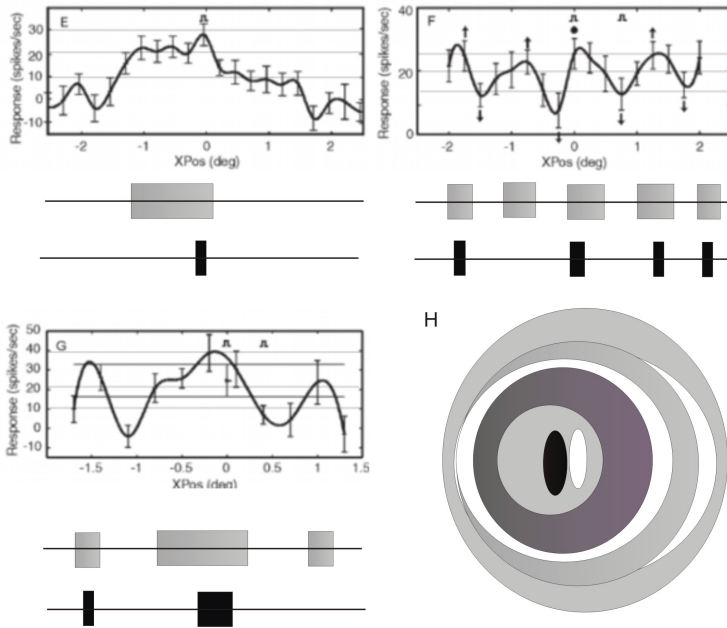


Fig. 4. Modified plots from [2]. Curves represent responses of several cells from area V4 to small single (E) and double (F, G) vertical bars. Bars change their position along x-axis (Xpos). Responses are measured in spikes/sec. Mean cell responses \pm SE are marked in E, F, and G. Cell responses are divided into three ranges by thin horizontal lines. Below each plot are schematics showing bar positions giving r_1 (gray) and r_2 (black) responses; below (E) for a single bar, below (F and G) for double bars (one bar was always in position 0). (H) This schematic extends responses for horizontally placed bars (E) to the whole RF: white color shows excitatory, black color inhibitory interactions between bars. Bars' interactions are asymmetric in the RF.

Table 2. Decision table for cells shown in Fig. 4. Attributes *o*, *ob*, *sf*, *sfb* were constant and are not presented in the table.

<i>cell</i>	<i>xp</i>	<i>xpr</i>	<i>xs</i>	<i>ys</i>	<i>s</i>	<i>r</i>
61e	-0.7	1.4	0.25	4	2	1
61f1	-1.9	0.2	0.25	4	22	2
61f2	0.1	0.2	0.25	4	22	2
61f3	1.5	0.1	0.25	4	22	2
61f4	-1.8	0.6	0.25	4	12	1
61f5	-0.4	0.8	0.25	4	22	1
61f6	0.4	0.8	0.25	4	22	1
61f7	1.2	0.8	0.25	4	22	1
62g1	-1.5	0.1	0.25	4	22	2
62g2	-0.15	0.5	0.25	4	22	2
62g3	-1.5	0.6	0.25	4	22	1
62g4	-0.25	1.3	0.25	4	22	1
62g5	1	0.6	0.25	4	22	1
63h1	-0.5	0	0.5	1	44	2
63h2	1	1	1	1	44	1
63h3	0.2	0.1	0.25	4	22	2

Table 3. Decision table for one cell shown in Fig. 5. Attributes *yp*, *yp_r* are constant and are not presented in the table. We introduce another parameter of the stimulus, difference in the direction of drifting grating of two patches: *ddg* = 0 when drifting are in the same directions, and *ddg* = 1 if drifting in two patches are in opposite directions.

<i>cell</i>	<i>xp</i>	<i>xpr</i>	<i>xs</i>	<i>ys</i>	<i>ddg</i>	<i>r</i>
64c	-4.5	3	1	1	1	2
64c1	-1.75	1.5	1	1	1	1
64c2	-0.5	1	1	1	1	2
64d	-6	0	1	8	0	2
64d1	-3.5	4.8	1	8	0	1

axons connections. As mentioned above, V4 axons in V1 have distinct clusters or linear branches. Descending pathways are modulators, which means that they follow the logical “or” rule. This rule states that cells in area V1 become more active as a result of the feedback only if their patterns “fit” to the area V4 cell “expectation”.

The decision table (Table 3) based on Fig. 5 describes cell responses to two patches placed in different positions along x-axis of the receptive field (RF). Figure 5 shows that adding the second patch reduced single patch cell responses. We have assumed that cell response to a single patch placed in the middle of the RF is *r*₂. The second patch suppresses cell responses to a greater extent when it is more similar to the first patch (Fig. 5D).

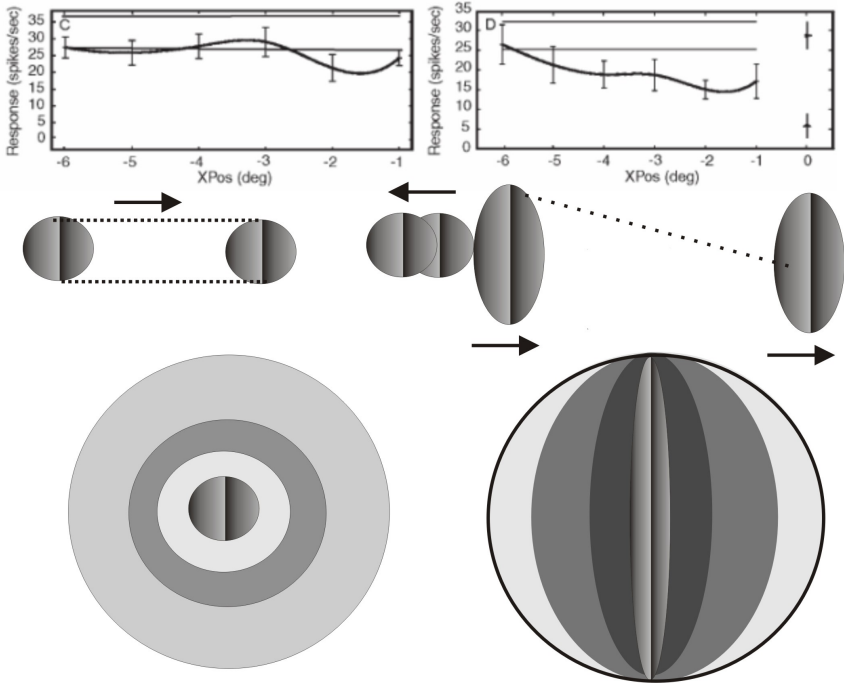


Fig. 5. Modified plots from [2]. Curves represent V4 cell responses to two patches with gratings moving in opposite direction - patch 1 deg diameter (C) and in the same (D) directions for patch 1 deg wide and 8 deg long. One patch is always at x-axis position 0 and the second patch changes its position as it is marked in *XPos* coordinates. The horizontal lines represent 95% confidence intervals for the response to a single patch in position 0. Below C and D, schematics show the positions of the patches and their influences on cell responses. Arrows are showing the direction of moving gratings. The lower part of the figure shows two schematics of the excitatory (white) and inhibitory (black) interactions between patches in the RF. Patches with gratings moving in the same directions (right schematic) show larger inhibitory areas (more dark color) than patches moving in opposite directions (left schematic).

Two-patch horizontal interaction decision rules are as follows:

DRT_V4_3:

$$ddg_1 \wedge (o_0 \wedge xpr_3 \wedge xp_{4.5} \wedge xs_1 \wedge ys_1)_1 \wedge (o_0 \wedge xp_0 \wedge xs_1 \wedge ys_1)_0 \rightarrow r_2 \quad (21)$$

DRT_V4_4:

$$ddg_1 \wedge (o_0 \wedge xpr_1 \wedge xp_{0.5} \wedge xs_1 \wedge ys_1)_1 \wedge (o_0 \wedge xp_0 \wedge xs_1 \wedge ys_1)_0 \rightarrow r_2 \quad (22)$$

DRT_V4_5:

$$ddg_0 \wedge (o_0 \wedge xpr_{4.8} \wedge xp_{3.5} \wedge xs_1 \wedge ys_8)_1 \wedge (o_0 \wedge xp_0 \wedge xs_1 \wedge ys_1)_0 \rightarrow r_1 \quad (23)$$

Table 4. Decision table for cells in Fig. 6. Attributes $yp, ypr, xs = ys = 0.5deg, s = 33$ (two discs) are constant and are not presented in the table. We introduce another parameter of the stimulus, difference in polarities of two patches: $dp = 0$ if polarities are same, and $dp = 1$ if polarities are opposite.

<i>cell</i>	<i>xp</i>	<i>xpr</i>	<i>dp</i>	<i>r</i>
81a	-0.1	0.5	0	1
81a1	-1.75	0.3	0	1
81a2	-1.2	1	1	1
81a3	1.25	1.5	1	1
81a4	-1.3	0.3	1	2
81a5	-1.3	0.3	1	2
81a6	1.5	0.4	1	2
81b	-1.4	0.6	1	1
81b1	0.9	0.8	1	1
81b2	0.9	0.2	1	2

These decision rules can be interpreted as follows: patches with drifting in opposite directions gratings give strong responses when positioned very near (overlapping) or 150% of their width apart one from the other eqs. (21, 22). Interaction of patches with a similar grating evoked small responses in large extend of the RF eq. (23).

Generally, interactions between similar stimuli evoke stronger and more extended inhibition than between different stimuli. These and other examples can be generalized to other classes of objects.

Two-spot horizontal interaction decision rules are as follows:

DRT_V4_6:

$$dp_0 \wedge s_{33} \wedge (((xp_{-0.1} \wedge xpr_{0.5}) \vee (xp_{-1.75} \wedge xpr_{0.3})) \wedge xs_{0.5})_1 \wedge (xp_0 \wedge xs_{0.5})_0 \rightarrow r_1 \quad (24)$$

DRT_V4_7:

$$dp_1 \wedge s_{33} \wedge (((xp_{-1.2} \wedge xpr_1) \vee (xp_{1.25} \wedge xpr_{1.5})) \wedge xs_{0.5})_1 \wedge (xp_0 \wedge xs_{0.5})_0 \rightarrow r_1 \quad (25)$$

DRT_V4_8:

$$dp_1 \wedge s_{33} \wedge (((xp_{-1.3} \wedge xpr_{0.2}) \vee (xp_{1.5} \wedge xpr_{0.4})) \wedge xs_{0.5})_1 \wedge (xp_0 \wedge xs_{0.5})_0 \rightarrow r_2 \quad (26)$$

DRT_V4_9:

$$dp_1 \wedge s_{33} \wedge (((xp_{-1.4} \wedge xpr_{0.6}) \vee (xp_{0.9} \wedge xpr_{0.8})) \wedge xs_{0.5})_1 \wedge (xp_0 \wedge xs_{0.5})_0 \rightarrow r_1 \quad (27)$$

DRT_V4_10:

$$dp_1 \wedge s_{33} \wedge ((xp_{0.9} \wedge xpr_{0.2}) \wedge xs_{0.5})_1 \wedge (xp_0 \wedge xs_{0.5})_0 \rightarrow r_2 \quad (28)$$

where dp is the difference in light polarities between two light spots (s_{33}), and subscript 1 is related to spot changing its x-axis position, whereas subscript 0 is related to the spot in 0 position on x-axis.

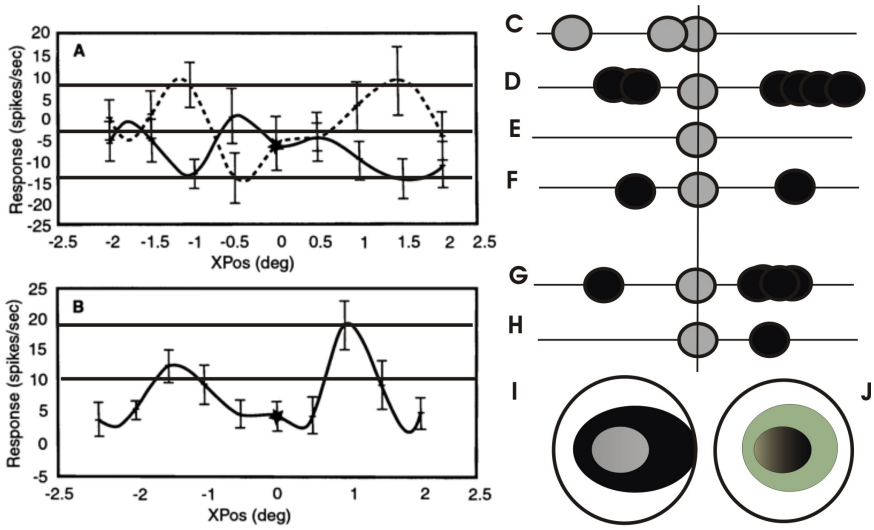


Fig. 6. Modified plots from [2]. Curves represent V4 cell responses to pair of 0.5 deg diameter bright and dark discs tested along width axis. Continuous lines mark the curves for responses to different polarity stimuli, and the same polarity stimuli are marked by dashed line. Schematics for cell responses showed in (A) are in (C-F) and (I, J). Schematics for cell responses in (B) are in (G) and (H). Interactions between same polarity light spots (C) are different than interactions between different polarities patches (D-H). Small responses (*class 1*) are in (C), (D), (G), and larger responses (*class 2*) are in (E), (F), (H). (E) shows that there is no r_2 responses in same polarity two spots interactions. (I) shows small excitatory (gray) in a short range and strong inhibitory (black) interactions between same polarity spots and (J) shows short range inhibitory (dark) and longer range excitatory interactions between different polarities spots.

We propose the following classes of the object’s **Parts Interaction Rules:**

- PIR1:** Facilitation when stimulus consists of multiple similar thin bars with small distances (about 0.5 deg) between them, and suppression when the distance between bars is larger than 0.5 deg. Suppression/facilitation is very often a nonlinear function of the distance. In our experiments (Fig. 3), cell responses to two bars were periodic along the receptive field with dominating periods of about 30, 50, or 70% of the RF width. These nonlinear interactions were also observed along vertical and diagonals of the RF and often show strong asymmetries in relationship to the RF middle.
- PIR2:** Strong inhibition when stimulus consists of multiple similar patches filled with gratings with the distance between patch edges ranging from 0 deg (touching) to 2 deg, weak inhibition when distance is between 3 to 5 deg through the RF width.

PIR3: If bars or patches have different attributes like polarity or drifting directions, their suppression is smaller and localized facilitation at the small distance between stimuli is present. As in bar interaction, suppression/facilitations between patches or bright/dark discs can be periodic along different RF axis and often asymmetric in the RF.

We have tested the above rules in nine cells from area V4 by using discs or annuli filled stimuli with optimally oriented and variable in spatial frequencies drifting gratings (Pollen et al. [2] Figs. 9, 10). Our assumptions were that if it is a strong inhibitory mechanism as described in the rule PRI2 then responses to annulus with at least 2 deg inner diameters will be stronger than responses to the disc. In addition by changing spatial frequencies of gratings inside the annulus, we have expected eventually to find other periodicities along the RF width as described by PIR3.

In summary, we wanted to find out what relations there are between stimulus properties and area V4 cell responses or whether B-elementary granules have equivalence classes of the relation $IND\{r\}$ or V4-elementary granules, or whether $[u]_B \Rightarrow [u]_{B4}$. It was evident from the beginning that because different area V4 cells have different properties, their responses to the same stimuli will be different, therefore we wanted to know if the rough set theory will help us in our data modeling.

We assign the spatial frequency: low (sf_l), medium (sf_m), and high (sf_h) as follows: sf_l if ($sf : 0 < sf \leq 1c/deg$), medium sf_m if ($sf : 1c/deg < sf \leq 4c/deg$), high sf_h if ($sf : sf > 4c/deg$). On the basis of this definition we calculate for each row in Table 5 the spatial frequency range by taking into account the spatial frequency bandwidth (sf_b). Therefore 107a is divided to 107al and 107am, 108a to 108al and 108am, and 108b to 108bl, 108bm, and 108bh.

Stimuli used in these experiments can be placed in the following ten categories:

$$\begin{aligned}
 Y_0 &= |sf_l \ xo_7 \ xi_0 \ s_4| = \{101, 105\} \\
 Y_1 &= |sf_l \ xo_7 \ xi_2 \ s_5| = \{101a, 105a\} \\
 Y_2 &= |sf_l \ xo_8 \ xi_0 \ s_4| = \{102, 104\} \\
 Y_3 &= |sf_l \ xo_8 \ xi_3 \ s_5| = \{102a, 104a\} \\
 Y_4 &= |sf_l \ xo_6 \ xi_0 \ s_4| = \{103, 106, 107, 108, 20a, 20b\} \\
 Y_5 &= |sf_l \ xo_6 \ xi_2 \ s_5| = \{103a, 106a, 107al, 108bl\} \\
 Y_6 &= |sf_l \ xo_4 \ xi_0 \ s_4| = \{108al\} \\
 Y_7 &= |sf_m \ xo_6 \ xi_2 \ s_5| = \{107am, 108bm\} \\
 Y_8 &= |sf_m \ xo_4 \ xi_0 \ s_4| = \{107a, 108am\} \\
 Y_9 &= |sf_h \ xo_6 \ xi_2 \ s_5| = \{108bh\}
 \end{aligned}$$

Table 5. Decision table for eight cells comparing the center-surround interaction. All stimuli were concentric, and therefore attributes were not xs, ys , but xo outer diameter, xi inner diameter. All stimuli were localized around the middle of the receptive field so that $xp = yp = xpr = ypr = 0$ were constant and we did not put them in the table. The optimal orientation were normalized, denoted as 1, and removed from the table.

<i>cell</i>	<i>sf</i>	<i>sfb</i>	<i>xo</i>	<i>xi</i>	<i>s</i>	<i>r</i>
101	0.5	0	7	0	4	0
101a	0.5	0	7	2	5	1
102	0.5	0	8	0	4	0
102a	0.5	0	8	3	5	0
103	0.5	0	6	0	4	0
103a	0.5	0	6	2	5	1
104	0.5	0	8	0	4	0
104a	0.5	0	8	3	5	2
105	0.5	0	7	0	4	0
105a	0.5	0	7	2	5	1
106	0.5	0	6	0	4	1
106a	0.5	0	6	3	5	2
107	0.5	0.25	6	0	4	2
107a	2.1	3.8	6	2	5	2
107b	2	0	4	0	4	1
108	0.5	0	6	0	4	1
108a	2	0	4	0	4	2
108b	5	9	6	2	5	2
20a	0.5	0	6	0	4	1
20b	0.5	0	6	0	4	2

These are equivalence classes for stimulus attributes, which means that in each class they are indiscernible $IND(B)$. We have normalized orientation bandwidth to 0 in $\{20a, 20b\}$ and spatial frequency bandwidth to 0, in cases $\{107, 107a, 108a, 108b\}$, and put values covered by the bandwidth to the spatial frequency parameters. There are three ranges of responses denoted as r_o, r_1, r_2 . Therefore on the basis of the neurological data there are the following three categories of cell responses:

$$|r_o| = \{101, 102, 102a, 103, 104, 105\}$$

$$|r_1| = \{101a, 103a, 105a, 107b, 108, 20a\}$$

$$|r_2| = \{104a, 106a, 107, 107al, 107am, 108al, 108am, 108bl, 108bm, 108bh, 20b\}$$

which are denoted as X_o, X_1, X_2 .

We will calculate the lower and upper approximation [1] of the brains basic concepts in term of stimulus basic categories:

$$\underline{B} X_0 = Y_0 \cup Y_2 = \{101, 105, 102, 104\}$$

$$\overline{B} X_0 = Y_0 \cup Y_2 \cup Y_3 \cup Y_4 = \{101, 105, 102, 104, 102a, 104a, 103, 106, 107, 108, 20a, 20b\}$$

$$\underline{B} X_1 = Y_1 = \{101a, 105a\}$$

$$\overline{B} X_1 = Y_1 \cup Y_5 \cup Y_6 \cup Y_4 =$$

$$\{101a, 105a, 103a, 107al, 108b, 106a, 20b, 107b, 108a, 103, 107, 106, 108, 20a\}$$

$$B X_2 = Y_7 \cup Y_9 = \{107am, 108bm, 108bh\}$$

$$\bar{B}X_2 = Y_7 \cup Y_9 \cup Y_8 \cup Y_6 \cup Y_3 \cup Y_4 \cup Y_5 = \{107am, 108bm, 108bh, 107b, 108am, 102a, 104a, 103a, 107a, 108bl, 106a, 20b, 103, 107, 106, 108, 20a, 108al\}$$

Concept 0 and concept 1 are roughly *B-defined*, which means that only with some approximation we have found that the stimuli do not evoke a response, or evoke weak or strong response in the area V4 cells. Certainly a stimulus such as Y_0 or Y_2 does not evoke a response in all our examples, in cells 101, 105, 102, 104. Also stimulus Y_1 evokes a weak response in all our examples: 101a, 105a. We are interested in stimuli that evoke strong responses because they are specific for area V4 cells. We find two such stimuli, Y_7 and Y_9 . In the meantime other stimuli such as Y_3, Y_4 evoke no response, weak or strong responses in our data.

We can find the quality [1] of our experiments by comparing properly classified stimuli $POSB(r) = \{101, 101a, 105, 105a, 102, 104, 107am, 108bm, 108bh\}$ to all stimuli and to all responses: $\gamma\{r\} = \frac{card\{101, 101a, 105, 105a, 102, 104, 107am, 108bm, 108bh\}}{card\{101, 101a, 20a, 20b\}} = 0.38$. We can also ask what percentage of cells we fully classified. We obtain consistent responses from 2 of 9 cells, which means that $\gamma = 0.22$. This is related to the fact that for some cells we have tested more than two stimuli. What is also important from an electrophysiological point of view is there are negative cases. There are many negative instances for the concept 0, which means that in many cases this brain area responds to our stimuli; however it seems that our concepts are still only roughly defined.

We have following decision rules:

DR_V4_7:

$$sf_l \wedge xo_7 \wedge xi_2 \wedge s_5 \rightarrow r_1 \quad (29)$$

DR_V4_8:

$$sf_l \wedge xo_7 \wedge xi_0 \wedge s_4 \rightarrow r_0 \quad (30)$$

DR_V4_9:

$$sf_l \wedge xo_8 \wedge xi_0 \wedge s_4 \rightarrow r_0 \quad (31)$$

DR_V4_10:

$$(sf_m \vee sf_h) \wedge xo_6 \wedge xi_2 \wedge s_5 \rightarrow r_2 \quad (32)$$

These can be interpreted as the statement that a large annulus (s_5) evokes a weak response, but a large disc (s_4) evokes no response when there is modulation with low spatial frequency gratings. However, somewhat smaller annulus containing medium or high spatial frequency objects evokes strong responses. It is unexpected that certain stimuli evoke inconsistent responses in different cells (Table 5):

$$103: sf_l \wedge xo_6 \wedge xi_0 \wedge s_4 \rightarrow r_0$$

$$106: sf_l \wedge xo_6 \wedge xi_0 \wedge s_4 \rightarrow r_1$$

$$107: sf_l \wedge xo_6 \wedge xi_0 \wedge s_4 \rightarrow r_2$$

A disc with not very large dimension containing a low spatial frequency grating can evoke no response (103), a small response (106), or a strong response (107).

4 Discussion

Physical properties of objects are different from their psychological representation. Gordenfors [27] proposed to describe the principle of human perceptual system as grouping objects by similarities in the conceptual space. Human perceptual systems group together similar objects with unsharp boundaries [27], which means that objects are related to their parts by rough inclusion or that different parts belong to objects with some approximation (degree) [28]. We suggest that similarity relations between objects and their parts are related to the hierarchical relationships between different visual areas. These similarities may be related to synchronizations of multi-resolution, parallel computations and are difficult to simulate using a digital computer [29].

Treisman [30] proposed that our brains extract features related to different objects using two different procedures: parallel and serial processing. The “basic features” were identified in psychophysical experiments as elementary features that can be extracted in parallel. Evidence of parallel features extraction comes from experiments showing that the extraction time becomes independent of the number of objects. Other features need serial searches, so that the extraction time is proportional to the number of objects. High-level serial processing is associated with integration and consolidation of items combined with conscious awareness. Other low-level parallel processes are rapid, global, related to high-efficiency categorization of items and largely unconscious [30]. Treisman [30] showed that instances of a disjunctive set of at least four basic features could be detected through parallel processing. Other researchers have provided evidence for parallel detection of more complex features, such as shape from shading [31] or experience-based learning of features of intermediate complexity [32].

Thorpe et al. [33] in recent experiments, however, found that human and non-human primates can rapidly and accurately categorize briefly flashed natural images. Human and monkey observers are very good at deciding whether or not a novel image contains an animal even when more than one image is presented simultaneously [34]. The underlying visual processing reflecting the decision that a target was present is under $150ms$ [33]. These findings are in contradiction to the classical view that only simple, “basic features”, likely related to early visual areas like V1 and V2, are processed in parallel [30]. Certainly, natural scenes contain more complex stimuli than “simple” geometric shapes. It seems that the conventional, two-stage perception-processing model needs correction, because to the “basic features” we must add a set of unknown intermediate features. We propose that at least some intermediate features are related to receptive field properties in area V4. Area V4 has been associated with shape processing because its neurons respond to shapes [35] and because lesions in this area disrupt shape discrimination, complex-grouping discriminations [36], multiple viewpoint shape discriminations [37], and rotated shape discriminations [38]. Area V4 responses are also driven by curvature or circularity, which was recently observed by mean of the human fMRI [39].

By applying rough sets to V4 neuron responses, we have differentiated between bottom-up information (hypothesis testing) related to the sensory input,

and predictions, some of which can be learned but are generally related to positive feedback from higher areas. If a prediction is in agreement with a hypothesis, object classification will change from category 1 to category 2. Our research suggests that such decisions can be made very effectively during pre-attentive, parallel processing in multiple visual areas. In addition, we found that the decision rules of different neurons can be inconsistent.

One should take into account that modeling complex phenomena demands the use of local models (captured by local agents), if one would like to use the multi-agent terminology [6]) that should be fused afterwards. This process involves negotiations between agents [6] to resolve contradictions and conflicts in local modeling. One of the possible approaches in developing methods for complex concept approximations can be based on the layered learning [41]. Inducing concept approximation should be developed hierarchically starting from concepts that can be directly approximated using sensor measurements toward complex target concepts related to perception. This general idea can be realized using additional domain knowledge represented in natural language.

We have proposed decision rules for different visual areas and for FF and FB connections between them. However in processing our V4 experimental data, we also have found inconsistent decision rules. These inconsistencies could help process different aspects of the properties of complex objects. The principle is similar to that observed in the orientation tuning cells of the primary visual cortex. Neurons in V1 with overlapping receptive fields show different preferred orientations. It is assumed that this overlap helps extract local orientations in different parts of an object. However, it is still not clear which cell will dominate if several cells with overlapping receptive fields are tuned to different attributes of a stimulus. Most models assume a “winner takes all” strategy; meaning that using a convergence (synaptic weighted averaging) mechanism, the most dominant cells will take control over other cells, and less represented features will be lost. This approach is equivalent to the two-valued logic implementation. Our finding from area V4 seems to support a different strategy than the “winner takes all” approach. It seems that different features are processed in parallel and then compared with the initial hypothesis in higher visual areas. We think that descending pathways play a major role in this verification process. At first, the activity of a single cell is compared with the feedback modulator by logical conjunction to avoid hallucinations. Next, the global, logical disjunction (“modulators”) operation allows the brain to choose a preferred pattern from the activities of different cells. This process of choosing the right pattern may have strong anatomical basis because individual axons have variable and complex terminal shapes, facilitating some regions and features against other so called salient features (for example Fig. 2). Learning can probably modify the synaptic weights of the feedback boutons, fine-tuning the modulatory effects of feedback.

Neurons in area V4 integrate an object’s attributes from the properties of its parts in two ways: (1) within the area via horizontal or intra-laminar local excitatory-inhibitory interactions, (2) between areas via feedback connections tuned to lower visual areas. Our research put more emphasis on feedback

connections because they are probably faster than horizontal interactions [42]. Different neurons have different Part Interactions Rules (PIR as described in the Results section) and perceive objects by way of multiple “unsharp windows” (Figs. 4, 6). If an object’s attributes fit the unsharp window, a neuron sends positive feedback [3] to lower areas, which as described above, use “modulator logical rules” to sharpen the attribute-extracting window and therefore change the neurons response from class 1 to class 2 (Fig. 4 J and K; Fig. 6 C to D, E to F, and G to H). The above analysis of our experimental data leads us to suggest that the central nervous system chiefly uses at least two different logical rules: “driver logical rule” and “modulator logical rule.” The first, “driver logical rule,” processes data using a large number of possible algorithms (over-representation). The second, “modulator logical rule,” supervises decisions and chooses the right algorithm.

Below we will look at possible cognitive interpretations of our model using the shape categorization task as an example. The classification of different objects by their different attributes has been regarded as a single process termed “subordinate classification” [40]. Relevant perceptual information is related to subordinate-level shape classification by distinctive information of the object like its size, surface, curvature of contours, etc. There are two theoretical approaches regarding shape representation: metric templates and invariant parts models. As mentioned above, both theories assume that an image of the object is represented in terms of cell activation in areas like V1: a spatially arrayed set of multi-scale, multi-oriented detectors (“Gabor jets”). Metric templates [26] map object values directly onto units in an object layer, or onto hidden units, which can be trained to differentially activate or inhibit object units in the next layer [41]. Metric templates preserve the metrics of the input without the extraction of edges, viewpoint invariant properties, parts or the relations among parts. This model discriminates shape similarities and human psychophysical similarities of complex shapes or faces [25]. Matching a new image against those in the database is done by allowing the Gabor jets to independently change their own best fit (change their position). The similarities of two objects will be the sum of the correlations in corresponding jets. When this method is used, changes in object or face position or changes in facial expressions can achieve 95% accuracy between several hundreds faces [43]. The main problems with the Lades model [26] described above are that it does not distinguish among the largest effects in object recognition it is insensitive to contour variations, which are very important psychophysically speaking, and it is insensitive to salient features (non-accidental properties [NAP]) [3].

The model we propose here suggests that these features are probably related to effects of feedback pathways, which may strengthen differences, signal salient features and also assemble other features, making it possible to extract contours. A geon structural description (GSD) is a two-dimensional representation of an arrangement of parts, each specified in terms of its non-accidental characterization and the relations amongst these parts [38]. Across objects, the parts (geons) can differ in their NAP. NAP are properties that do not change with

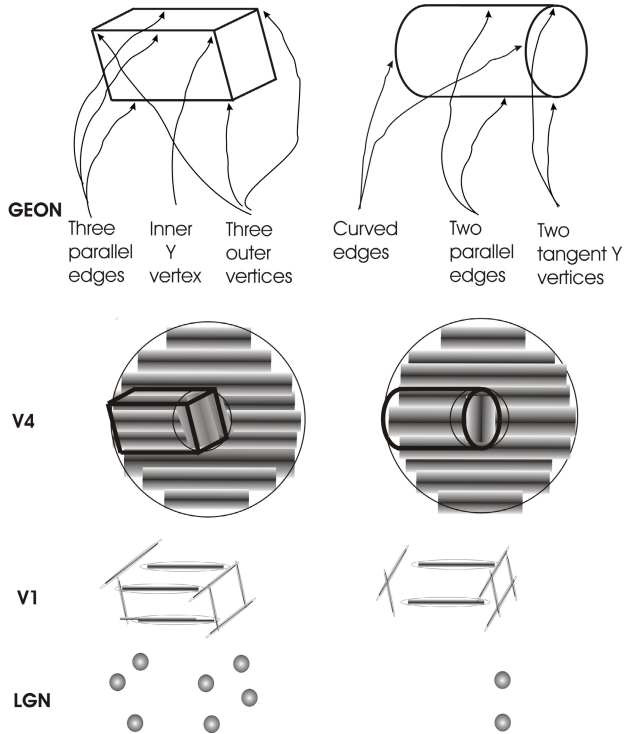


Fig. 7. Comparison of differences in nonaccidental properties between a brick and a cylinder using geon [3] and our model. The geon shows attributes from psychological space like curves, parallels or vertices, which may be different in different subjects. The neurological model compares properties of both objects on the basis of a single cell recordings from the visual system. Both objects can stimulate similar receptive fields in area V4. These receptive fields are sensitive in annuli - they extract orientation change in different parts of the RF [2]. Area V1 RFs are sensitive to edge orientations, whereas LGN RFs extract spots related to corners. All these different attributes are put together by FF and FB pathways.

small depth rotations of an object. The presence or absence of the NAP of some geons or the different relations between them may be the basis for subordinate level discrimination [38]. The advantage of the GSD is that the representation of objects in terms of their parts and the relations between them is accessible to cognition and fundamental for viewpoint invariant perception. Our neurological model introduces interactions between RF parts as in the geon model; however, our parts are defined differently than the somewhat subjective parts of the GSD model. Fig. 7 shows differences in a simple objects understanding between geon and our neurological approach. The top part of this figure shows differences in nonaccidental properties between a brick and a cylinder [3]. We propose hierarchical definition of parts based on neurophysiological recordings from the visual system. Both objects may be classified in V4 by the receptive field discriminating

between different stimulus orientations in its central and peripheral parts as it is schematically presented in Fig. 7 [2]. Another, different classification is performed by area V1, where oriented edges are extracted from both objects (Fig. 7). However, even more precise classification is performed in LGN where objects are seen as sets of small circular shapes similar to receptive fields in the retina (bottom part of Fig. 7).

In our model, interactions between parts and NAPs are associated with the role of area V4 in visual discrimination, as described in the above lesion experiments [34–36]. However, feedback from area V4 to the LGN and area V1 could be responsible for the possible mechanism associated with the properties of the GSD model. The different interactions between parts may be related to the complexity and the individual shapes of different axons descending from V4. Their separated cluster terminals may be responsible for invariance related to small rotations (NAP). These are the anatomical bases of the GSD model, although we hypothesize that the electrophysiological properties of the descending pathways (FB), defined above as the modulator, are even more important. The modulating role of the FB is related to the anatomical properties of the descending pathways' logic. Through this logic, multiple patterns of the coincidental activity between the LGN or V1 and FB can be extracted. One may imagine that these differently extracted patterns of activity correlate with the multiple viewpoints or shape rotations defined as NAP in the GSD model.

In summary, by applying rough set theory to model neurophysiological data we have shown a new approach for objects categorization in psychophysical space. Two different logical rules are applied to indiscernibility classes of LGN, V1, and V4 receptive fields: “driver logical rules” put many possible objects' properties together and “modulator logical rules” choose these attributes which are in agreement with our previous experiences.

Acknowledgement. Thanks to Carmelo Milo for his technical help, as well to Farah Averill and Dana Hayward for their help in editing the manuscript.

References

1. Pawlak, Z.: *Rough Sets - Theoretical Aspects of Reasoning about Data*. Kluwer Academic Publishers, Dordrecht (1991)
2. Pollen, D.A., Przybyszewski, A.W., Rubin, M.A., Foote, W.: Spatial receptive field organization of macaque V4 neurons. *Cereb Cortex* 12, 601–616 (2002)
3. Biederman, I.: Recognition-by-components: a theory of human image understanding. *Psychol. Rev.* 94(2), 115–147 (1987)
4. Przybyszewski, A.W., Gaska, J.P., Foote, W., Pollen, D.A.: Striate cortex increases contrast gain of macaque LGN neurons. *Vis. Neurosci.* 17, 485–494 (2000)
5. Przybyszewski, A.W., Kagan, I., Snodderly, M.: Eye position influences contrast responses in V1 of alert monkey [Abstract]. *Journal of Vision* 3(9), 698, 698a (2003), <http://journalofvision.org/3/9/698/>
6. Russell, S., Norvig, P.: *Artificial Intelligence: A Modern Approach*, 2nd edn. Prentice Hall Series in Artificial Intelligence (2003)

7. Przybyszewski, A.W., Kon, M.A.: Synchronization-based model of the visual system supports recognition. Program No. 718.11. 2003 Abstract Viewer/Itinerary Planner. Society for Neuroscience, Washington, DC (2003)
8. Kuffler, S.W.: Neurons in the retina; organization, inhibition and excitation problems. *Cold Spring Harb. Symp. Quant. Biol.* 17, 281–292 (1952)
9. Hubel, D.H., Wiesel, T.N.: Receptive fields, binocular interaction and functional architecture in the cat's visual cortex. *J. Physiol.* 160, 106–154 (1962)
10. Schiller, P.H., Finlay, B.L., Volman, S.F.: Quantitative studies of single-cell properties in monkey striate cortex. I. Spatiotemporal organization of receptive fields. *J. Neurophysiol.* 39, 1288–1319 (1976)
11. Kagan, I., Gur, M., Snodderly, D.M.: Spatial organization of receptive fields of V1 neurons of alert monkeys: comparison with responses to gratings. *J. Neurophysiol.* 88, 2557–2574 (2002)
12. Bardy, C., Huang, J.Y., Wang, C., FitzGibbon, T., Dreher, B.: 'Simplification' of responses of complex cells in cat striate cortex: suppressive surrounds and 'feedback' inactivation. *J. Physiol.* 574, 731–750 (2006)
13. Przybyszewski, A.W.: Checking Brain Expertise Using Rough Set Theory. In: Kryszkiewicz, M., Peters, J.F., Rybinski, H., Skowron, A. (eds.) RSEISP 2007. LNCS (LNAI), vol. 4585, pp. 746–755. Springer, Heidelberg (2007)
14. Alonso, J.M., Usrey, W.M., Reid, R.C.: Rules of connectivity between geniculate cells and simple cells in cat primary visual cortex. *J. Neurosci.* 21(11), 4002–4015 (2001)
15. Sherman, S.M., Guillery, R.W.: The role of the thalamus in the flow of information to the cortex. *Philos. Trans. R Soc. Lond. B Biol. Sci.* 357(1428), 1695–1708 (2002)
16. Lund, J.S., Lund, R.D., Hendrickson, A.E., Bunt, A.H., Fuchs, A.F.: The origin of efferent pathways from the primary visual cortex, area 17, of the macaque monkey as shown by retrograde transport of horseradish peroxidase. *J. Comp. Neurol.* 164, 287–303 (1975)
17. Fitzpatrick, D., Usrey, W.M., Schofield, B.R., Einstein, G.: The sublaminar organization of corticogeniculate neurons in layer 6 of macaque striate cortex. *Vis. Neurosci.* 11, 307–315 (1994)
18. Ichida, J.M., Casagrande, V.A.: Organization of the feedback pathway from striate cortex (V1) to the lateral geniculate nucleus (LGN) in the owl monkey (*Aotus trivirgatus*). *J. Comp. Neurol.* 454, 272–283 (2002)
19. Angelucci, A., Sainsbury, K.: Contribution of feedforward thalamic afferents and corticogeniculate feedback to the spatial summation area of macaque V1 and LGN. *J. Comp. Neurol.* 498, 330–351 (2006)
20. Nakamura, H., Gattass, R., Desimone, R., Ungerleider, L.G.: The modular organization of projections from areas V1 and V2 to areas V4 and TEO in macaques. *J. Neurosci.* 13, 3681–3691 (1993)
21. Rockland, K.S., Virga, A.: Organization of individual cortical axons projecting from area V1 (area 17) to V2 (area 18) in the macaque monkey. *Vis. Neurosci.* 4, 11–28 (1990)
22. Rockland, K.S.: Configuration, in serial reconstruction, of individual axons projecting from area V2 to V4 in the macaque monkey. *Cereb Cortex* 2, 353–374 (1992)
23. Rockland, K.S., Saleem, K.S., Tanaka, K.: Divergent feedback connections from areas V4 and TEO in the macaque. *Vis. Neurosci.* 11, 579–600 (1994)
24. Schummers, J., Mario, J., Sur, M.: Synaptic integration by V1 neurons depends on location within the orientation map. *Neuron* 36, 969–978 (2002)

25. Przybyszewski, A.W., Potapov, D.O., Rockland, K.S.: Feedback connections from area V4 to LGN. In: Ann. Meet. Society for Neuroscience, San Diego, USA (2001), <http://sfn.scholarone.com/itin2001/prog#620.9>
26. Lades, M., Vortbrueggen, J.C., Buhmann, J., Lange, J., von der Malsburg, C., Wurtz, R.P., Konen, W.: Distortion invariant object recognition in the dynamic link architecture. *IEEE Transactions on Computers* 42, 300–311 (1993)
27. Grdenfors, P.: *Conceptual Spaces*. MIT Press, Cambridge (2000)
28. Polkowski, L., Skowron, A.: Rough Mereological Calculi of Granules: A Rough Set Approach to Computation. *Computational Intelligence* 17, 472–492 (2001)
29. Przybyszewski, A.W., Linsay, P.S., Gaudiano, P., Wilson, C.: Basic Difference Between Brain and Computer: Integration of Asynchronous Processes Implemented as Hardware Model of the Retina. *IEEE Trans. Neural Networks* 18, 70–85 (2007)
30. Treisman, A.: Features and objects: the fourteenth Bartlett memorial lecture. *Q J. Exp. Psychol. A* 40, 201–237 (1988)
31. Ramachandran, V.S.: Perception of shape from shading. *Nature* 331, 163–166 (1988)
32. Ullman, S., Vidal-Naquet, M., Sali, E.: Visual features of intermediate complexity and their use in classification. *Nature Neuroscience* 5, 682–687 (2002)
33. Thorpe, S., Fize, D., Merlot, C.: Speed of processing in the human visual system. *Nature* 381, 520–522 (1996)
34. Rousselet, G.A., Fabre-Thorpe, M., Thorpe, S.J.: Parallel processing in high-level categorization of natural images. *Nat. Neurosci.* 5, 629–630 (2002)
35. David, S.V., Hayden, B.Y., Gallant, J.L.: Spectral receptive field properties explain shape selectivity in area V4. *J. Neurophysiol.* 96, 3492–3505 (2006)
36. Merigan, W.H.: Cortical area V4 is critical for certain texture discriminations, but this effect is not dependent on attention. *Vis. Neurosci.* 17(6), 949–958 (2000)
37. Merigan, W.H., Pham, H.A.: V4 lesions in macaques affect both single- and multiple-viewpoint shape discriminations. *Vis. Neurosci.* 15(2), 359–367 (1998)
38. Girard, P., Lomber, S.G., Bullier, J.: Shape discrimination deficits during reversible deactivation of area V4 in the macaque monkey. *Cereb Cortex* 12(11), 1146–1156 (2002)
39. Dumoulin, S.O., Hess, R.F.: Cortical specialization for concentric shape processing *Vision Research*, vol. 47, pp. 1608–1613 (2007)
40. Biederman, I., Subramaniam, S., Bar, M., Kalocsai, P., Fiser, J.: Subordinate-level object classification reexamined. *Psychol. Res.* 62, 131–153 (1999)
41. Poggio, T., Edelman, S.: A network that learns to recognize three-dimensional objects. *Nature* 343, 263–266 (1990)
42. Girard, P., Hup, J.M., Bullier, J.: Feedforward and feedback connections between areas V1 and V2 of the monkey have similar rapid conduction velocities. *J. Neurophysiol.* 85(3), 1328–1331 (2001)
43. Wiscott, L., Fellous, J.-M., Krueger, N., von der Malsburg, C.: Face recognition by elastic graph matching. *IEEE Pattern Recognition and Machine Intelligence* 19, 775–779 (1997)